SOILS AND FOUNDATIONS Vol. 41, No. 1, 57–67, Feb. 2001
Japanese Geotechnical Society

GROUND AND PILE-GROUP RESPONSES DUE TO TUNNELLING

N. LOGANATHAN[i], H. G. POULOS[ii] and K. J. XU[iii]

ABSTRACT

In urban areas, where many of the high-rise buildings are supported by pile foundations, the number of soft-ground tunnels has increased rapidly during recent years. To minimize the risk of damage as a result of tunnel construction the engineer who designs a tunnel needs to be able to make reliable predictions of the ground deformations induced by tunnelling and their effects on any adjacent pile foundations. In this paper, a closed form solution, developed by the authors, is used to assess the displacement field around the tunnel. The displacements estimated are then imposed on single piles and pile groups in simplified boundary element analyses to compute pile and pile group responses. The analytical method presented in this paper was verified with a case history and with numerical results obtained using FLAC^{3D} computer software. Comparisons are made to evaluate the group action for various pile group configurations. The influence of various pile lengths and pile locations from the tunnel is also presented.

Key words: boundary element method, ground deformation, ground loss, pile-group response, soft ground, tunnelling (**IGC**: E2/E13/H5)

INTRODUCTION

During the tunnelling process somewhat more soil is removed than the volume of the tunnel, leading to changes in the stress state of the soil. The influence of these changes on adjacent pile foundations is of importance when a bored tunnel is planned in an urban area where many structures are supported on pile foundations. Ground movements due to tunnelling may induce bending moments, lateral and vertical loads, and settlements and lateral deflections in the piles, which may lead to structural distress or failure of the piles or the super-structure.

The interaction between loaded foundation piles and a tunnel under construction is a three dimensional problem and modelling the influence of the tunnel is only possible if the tunnelling-induced ground movements are assessed accurately. In practice the tunnelling-induced ground movements are assessed by using empirical methods (Peck, 1969; Mair, 1993; Clough and Schmidt, 1981; O'Reilly and New, 1982), analytical methods (Sagaseta, 1987; Verruijt and Booker, 1996), and finite element methods (Gunn, 1993; Rowe and Kack, 1983). Each method is subject to some limitations.

To date, research work on the effects of tunnelling on piled foundations appears to be very limited, and the main purpose of the present study is to develop a better understanding of the behaviour of piles influenced by tunnelling operations. The main objectives of this paper are three-fold: first, to employ a closed-form analytical solution for ground movements developed by the authors; second, to introduce the applicability of the boundary element method in three dimensional modelling of the pile-soil interaction; and third, to assess the behaviour of a pile-group due to tunnelling-induced ground movement and to compare this with the behaviour of single pile at equal distance from the tunnel.

ANALYTICAL PREDICTION OF TUNNELLING-INDUCED GROUND MOVEMENTS

Excavation of a tunnel provides an opening into which the soil can deform. The movement of the soil into the opening can be related to the concept of "loss of ground," which is defined as volume of material (whether through the face or radial encroachment over and around or behind the shield) that has been excavated in excess of the theoretical design volume of excavation. In practice, as pointed out by Rowe and Kack (1983), the radial ground movement into the tunnel excavation is not uniform since the equivalent two dimensional (*2D*) gap 'g' (tail void) around the tunnel is noncircular (e.g., typically oval-shaped) as shown in Fig. 1(b). The possible reasons assumed for the formation of an oval-shaped gap around the tunnel are (1) tunnel operators advance the shield at a lightly upward pitch relative to the actual design grade to avoid the diving tendency of the shield (there is also a chance that the opposite behaviour occurs

[i] Senior Engineer (Geotechnical), PB Merz & McLellan Pte Ltd, 95 South Bridge Road, #08-18, Pidemco Centre, Singapore 058717.
[ii] Senior Principle, Coffey Geosciences Pty Ltd. and Professor of Civil Engineering, University of Sydney, Australia.
[iii] Research Assistant, Dept. of Civil Engineering, University of Sydney, Sydney, NSW 2006, Australia.
Manuscript was received for review on July 9, 1999.
Written discussions on this paper should be submitted before September 1, 2001 to the Japanese Geotechnical Society, Sugayama Bldg. 4F, Kanda Awaji-cho 2-23, Chiyoda-ku, Tokyo 101-0063, Japan. Upon request the closing date may be extended one month.

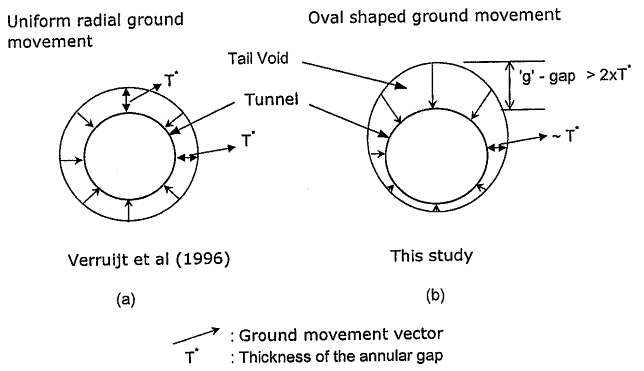

Fig. 1. Circular and oval-shaped ground deformation patterns around the tunnel section

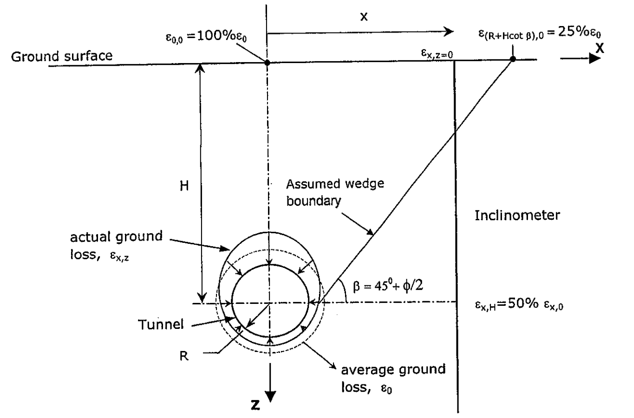

Fig. 2. Ground deformation patterns and the ground loss boundary conditions

since the behaviour of shield on pitching depends on various factors such as the ground condition, the type of shield etc.); (2) the tunnel lining settles on the bottom of the excavated ground when the tail piece is removed; and (3) three dimentional (3*D*) elastoplastic movement of the soil occurs at the tunnel face.

Verruijt and Booker (1996) presented closed-form solutions to estimate the tunnelling-induced ground deformations assuming uniform radial ground movement as shown in Fig. 1(a). In that paper, the ground loss estimated assuming the uniform radial ground movement (average ground loss) is denoted as, ε_0. In practice, the soil movement around the tunnel is non-uniform (due to the oval-shaped gap), and the ground loss parameter representing the oval-shaped gap is defined as, $\varepsilon_{x,z}$.

When the portion of the soil above the tunnel crown touches the tunnel lining, the soil at the side of the tunnel displaces towards the bottom of the tunnel. Therefore, the upward movement of the soil below the tunnel is limited. Centrifuge model tests carried out by Stallebrass et al. (1996) and Taylor (1998) have revealed similar results. When the tunnel lining settles on the bottom of the annulus gap (due to the self-weight), the distance between the crown of the excavated surface becomes twice the thickness of the annulus gap (Fig. 1). This condition may not occur when tunnel with large diameter under ground water level move upward due to buoyancy force. Boundary conditions derived based on the ground movement components are shown in Fig. 2 and detailed explanations are given in Loganathan and Poulos (1998). The equivalent average undrained ground loss (ε_0) is defined with respect to the gap parameter as shown in Eq. (1):

$$\varepsilon_0=\frac{\pi\left(R+\dfrac{g}{2}\right)^2-\pi R^2}{\pi R^2}\cdot 100\%=\frac{4gR+g^2}{4R^2}\cdot 100\% \qquad (1)$$

where R = the radius of the tunnel, and g = the gap estimated as shown in Appendix A. Before the formation of the gap, all the initial stresses in soil are in equilibrium. The stresses around the tunnel are released in a non-uniform manner due to the oval-shaped gap geometry. The movements of the surrounding soil into the gap due to the stress release determine the ground deformation pattern. In the present study, the ground loss parameter obtained in Eq. (1) is further modified in order to incorporate the non-uniform radial movement of the soil around the tunnel, which basically influences the deformation pattern of the surrounding soil. The equivalent ground loss parameter ($\varepsilon_{x,z=0}$) which causes the surface settlement may be derived by adopting an exponential function for the average equivalent ground loss parameter (ε_0), that models the non-uniform movement of the soil around the tunnel, as shown in Eq. (2):

$$\varepsilon_{x,z=0}=\varepsilon_0\cdot B\exp(-Ax^2) \qquad (2)$$

where A, B are constants and ε_0 is the average equivalent ground loss as obtained from Eq. (1). Constants A and B are derived based on the boundary conditions described below.

When the portion of the soil above the tunnel crown touches the tunnel lining, the soil at the side of the tunnel displaces towards the bottom of the tunnel. Therefore, the upward movement of the soil below the tunnel is limited. Centrifuge model tests carried out by Stallebrass et al. (1996) revealed similar results. In this study, it is assumed that about 75% of the vertical ground movement occurs within the upper annulus of the gap around the tunnel. Figure 2 shows the vertical ground movement influence zone where most of the soil displacements occur. The relationship between settlement trough width (which is an indirect measure of the ground movement influence zone) and the tunnel depth can be expressed as a vertical angle, β, drawn from the spring line of the tunnel to the width of the settlement trough at the surface. In sandy soil, the limit angle, β, is defined as $(45+\phi/2)$, where ϕ = angle of shearing resistance of the sand. For soft to stiff clay β may be assumed to be 45° based on the observations made by Cording and Hansmire (1975), i.e. it is assumed that the ground movement occurs predominantly within the 45° wedge in between the ground surface and the tunnel. Therefore, it may be assumed that the surface settlement above the tunnel axis is the resultant of the complete cumulative equivalent average ground loss (100% ε_0) around the tunnel and the surface settlement at the horizontal distance ($H+R\cot\beta$) is the resultant of partial cumulative equivalent average ground loss (25% ε_0). These boundary conditions are shown in Fig. 2.

By applying these boundary conditions (*see* Fig. 2) to Eq. (2), the equivalent ground loss component which models the non-uniform vertical movement is derived as shown in Eq. (3).

$$\varepsilon_{x,z=0}=\varepsilon_0 \exp\left[-\frac{1.38x^2}{(R+H\cot\beta)^2}\right] \tag{3}$$

where ε_0=average radial ground loss, H=tunnel depth, R=tunnel radius, x=lateral distance from tunnel centerline, β=limit angle=$(45+\varphi/2)$, and φ=angle of shearing resistance.

Observations made by Deane and Bassett (1995) and Stallebrass et al. (1996) show that the horizontal ground movement into the tail void or gap is a maximum at the spring line of the tunnel and is zero at the crown and the invert of the tunnel. The ground loss parameter $\varepsilon_{x,z}$, which causes the ground deformation around the tunnel may be derived by adopting an exponential function for the ground loss component which causes the ground settlement $\varepsilon_{x,z=0}$, and applying the boundary conditions shown in Fig. 2, as shown in Eq. (4):

$$\varepsilon_{x,z=0}=\varepsilon_0 \exp\left\{-\left[\frac{1.38x^2}{(R+H\cot\beta)^2}+\frac{0.69z^2}{H^2}\right]\right\} \tag{4}$$

A closed form solution has been presented by Verruijt and Booker (1996) but it has been found that this solution gives a much wider settlement trough than empirical methods and field measurements. The reason for this observation is the ground deformation at the tunnel soil interface may not be the uniform radial ground movement which the theory assumes. The writers have modified the Verruijt and Booker (1996) solutions to accommodate the newly defined ground loss parameter $\varepsilon_{x,z}$ (Eq. (4)) that incorporates the nonlinear ground movement around the tunnel soil interface. The duration of gap (tail void) formation is short and may be regarded as occurring under the undrained condition. Since this study is concerned only with short-term undrained conditions, the ground deformations due to long-term ovalization of the tunnel lining are not considered in this study. The generalized modified analytical solutions for the estimation of the surface settlement, sub-surface settlement and the lateral deformation are given in Eqs. (5), (6) and (7), respectively:

$$U_{z=0}=\varepsilon_0 R^2\cdot\frac{4H(1-\nu)}{H^2+x^2}\cdot\exp\left\{-\frac{1.38x^2}{(H\cot\beta+R)^2}\right\} \tag{5}$$

$$U_z=\varepsilon_0 R^2\left(-\frac{z-H}{x^2+(z-H)^2}+(3-4\nu)\frac{z+H}{x^2+(z+H)^2}-\frac{2z[x^2-(z+H)^2]}{[x^2+(z+H)^2]^2}\right)\cdot\exp\left\{-\left[\frac{1.38x^2}{(H\cot\beta+R)^2}+\frac{0.69z^2}{H^2}\right]\right\} \tag{6}$$

Table 1. Comparison of settlement trough width

Tunnel Depth/Diameter (H/D)	Settlement trough width, i				
	Loganathan & Poulos (1998)	Mair (1993)	Sagaseta (1987)	O'Reilly & New (1982)	Clough & Schmidt (1981)
18/6 (=3)	9.3	9.0	10.3	8.8	7.2
16/4 (=4)	8.0	8.0	9.2	8.0	6.1
25/5 (=5)	9.8	10.0	11.5	9.7	7.2
18/3 (=6)	8.7	9.0	10.3	8.8	6.3

$$U_x=-\varepsilon_0 R^2 x\left[\frac{1}{x^2+(H-z)^2}+\frac{(3-4\nu)}{x^2+(H+z)^2}-\frac{4z(z+H)}{(x^2+(H+z)^2)^2}\right]\cdot\exp\left\{-\left[\frac{1.38x^2}{(H\cot\beta+R)^2}+\frac{0.69z^2}{H^2}\right]\right\} \tag{7}$$

where $U_{z=0}$=ground surface settlement; U_z=sub-surface settlement; U_x=lateral soil movement; R=tunnel radius; z=depth below ground surfacc; H=depth of tunnel axis level; ν=Poisson's ratio of soil; ε_0=average ground loss ratio, and x=lateral distance from tunnel centerline.

These equations allow rapid estimation of the ground deformations and require only an estimate of the Poisson's ratio ν, of the soil. The applicability of these solutions has been evaluated with reference to a number of case histories (Loganathan and Poulos, 1998, 1999).

In empirical methods, the settlement trough width "i" is considered to be an important parameter in the determination of the surface settlements. The relationship obtained between the normalised parameters i/R and $H/2R$ parameters for the proposed analytical solution is shown in Eq. (8):

$$\frac{i}{R}=\frac{1.15}{(\tan\beta)^{0.35}}\left(\frac{H}{2R}\right)^{0.9/(\tan\beta)^{0.23}} \tag{8}$$

A comparison of the surface settlement trough width "i" parameter derived from various methods is shown in Table 1, and this shows that the predictions made using Eq. (8) are in good agreement with the values predicted using empirical relationships established by Mair (1993), and O'Reilly and New (1982).

The construction of a tunnel adjacent to existing piles requires a proper consideration of the pile response to the externally imposed soil movements due to tunnelling, and an assessment of the consequent axial movement, lateral deflection, bending moment and rotation of the pile head. Analyses based on simplified boundary element procedures have been used in this study, as described below.

MODELLING OF THREE DIMENSIONAL PILE-SOIL INTERACTION USING BOUNDARY ELEMENT METHOD

At present, various numerical approaches have been employed in estimating pile group responses due to combinations of external loading. Computer programs for the analysis of pile groups vary in the type of approach used and in the sophistication of treatment of different aspects of group behaviour. Among the most widely used general programs for pile group analysis are PGROUP (Benerjee, 1976), DEFPIG (Poulos, 1979, 1990), and PIGLET (Randolph, 1980). All these programs are based on elastic continuum analysis, although DEFPIG can also be extended into the non-linear range by specifying limiting values of skin friction and lateral pressure along the pile.

Although these programs have been used widely, they all involve simplifications and idealizations, including; (1) pile to pile interactions are used instead of individual pile element to pile element interactions, (2) the actual non uniform stress distributions around the pile (especially in the lateral loading case) are modified to an equivalent uniform stress distribution over each pile elements, (3) Load-deformation behaviour is modeled individually without considering the deformation coupling effects due to three dimensional loading, and (4) off-pile loading conditions arising from adjacent constructions such as embankments, excavations, tunnelling etc. are not considered.

A computer program GEPAN (GEneral Pile ANalysis) has been developed at Sydney University (Xu and Poulos, 1998) to eliminate the limitations and idealizations of the existing computer programs discussed above. A three dimensional boundary element analysis, together with the virtual image technique for an elastic half-space, have been used to carry out analyses of multiple single piles and pile groups which incorporate the effect of external soil movements due to embankments, tunnels and excavations. Figure 3 shows a typical pile element discretization used in the computer program GEPAN. The following assumptions are employed in the development of the three dimensional boundary element analyses:

1. Soil is assumed to be ideal homogeneous isotropic elastic weightless half-space, having elastic parameters E_s and ν_s that are not influences by the presence of the piles.
2. Piles are assumed to be circular in cross-section and to be composed of a homogeneous isotropic elastic material with two unchangeable elastic parameters. The piles are vertical and perfectly rough. Where the diameter of a pile changes abruptly, no account is taken of local stress concentration.
3. The deformations of piles and soil mass are elastic and the superposition principle is valid.
4. The boundary elements are meshed in partly cylindrical or ring surfaces. The distributions of the stress components on the boundary elements at the pile-soil interface are assumed to be uniform over each element.
5. The load and displacement components at the top of piles are average values.
6. The caps above pile groups are assumed to be rigid and free of the soil surface.
7. There is no slip at the pile-soil interface.

This programme automatically generates a group of unified geometry and control parameters based on the source data. Each pile is subjected to a total of six components of load.

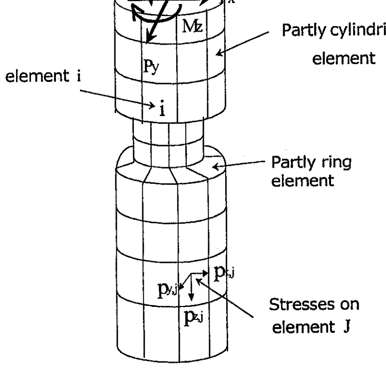

Fig. 3. Schematic diagram showing 3*D* boundary element discretization, external loads and surface stresses acting on a pile

More accurate pile load-deformation responses are obtained by assuming that load-deformation interaction occurs between each element of each pile of each group. Twelve kinds of influence factors are classified and presented by corresponding influence factor matrixes (IFM) which are of a hierarchical nature. The resulting global equation for pile response is shown in Eq. (9).

$$\begin{pmatrix} A & B & \phi & D \\ \phi & \phi & G & H \\ O & P & Q & R \\ S & \phi & \phi & V \end{pmatrix} \begin{pmatrix} X_e \\ X_b \\ X_c \\ X_t \end{pmatrix} = \begin{pmatrix} Y_q \\ Y_c \\ \phi \\ Y_p \end{pmatrix} \tag{9}$$

where A=IFM of element displacement and stress ($=SIF+PIF$), SIF=IFM of element soil displacement and stress, PIF=IFM of element pile displacement and stress, B=IFM of element displacement and pile tip displacement, D=IFM of element displacement and pile head load, G=IFM of cap displacement and cap-tie-cap beam force (to allow for pile caps jointed by tie beam, H=IFM of cap load and pile head load, O=IFM of pile head displacement and element stress, P=IFM of pile head displacement and pile tip displacement, Q=IFM of pile head displacement and cap displacement, R=IFM of pile head displacement and pile head load, S=IFM of pile head load and element stress, V=IFM of pile head load and pile head load, Y_q=vector of element stress offset ($=Y_{q,t}+Y_{q,e}$), $Y_{q,t}$=vector of element displacement due to pile head load, $Y_{q,e}$=vector of element displacement due extra soil displacement/stress/force, Y_c=vector of cap load, Y_p=vector of pile head load, X_e=vector of pile-soil stress, X_b=vector of pile tip displacement, X_c=vector of cap displacement, and X_t=vector of capped pile head force.

Details of the various matrices and vectors are given by

Xu and Poulos (1998). The global Eq. (9) contains the following four kinds of independent equations: compatibility equations at the pile-soil interfaces; equilibrium equations for pile heads and caps; compatibility equations for pile heads and caps; equilibrium equations for piles. In the global matrix, there are twelve influence factor matrixes (IFM), i.e. *SIF, PIF, B, D, G, H, O, P, Q, R, S, V*. There are four types of IFM according to the method of their derivation:

1. The IFM for displacement and stress on soil elements, *SIF*, is obtained by integration of the Mindlin's equation (Mindlin, 1936).
2. The IFM relating displacements due to stress or load on a pile, *PIF, D, G, R* is determined via the principles of structural analysis.
3. The IFM relating displacements among top, tip and elements on piles, *B, P, Q* are derived by the deformation geometry of the piles.
4. The IFM relating pile head load, load on the pile cap, or stress on piles, *H, S, V*, are established by force equilibrium.

The global foundation is assumed to contain NCAP pile groups with any configuration, NPILS non-identical piles which have NIPSUM individual piles and NCPSUM piles in groups, and NTOT elements with any size which may include partly cylindrical elements on shafts and partly ring elements on both bases and discontinuities. Then a coupled global matrix with [3*NTOT+6*NPILS+6*NCAP+6*NCPSUM] dimensions is set up, and the following unknowns can be solved:

1. 3*NTOT pile-soil stresses of elements $\{X_e\}$
2. 6*NIPLS tip displacements of piles $\{X_b\}$
3. 6*NCAP cap displacements of caps $\{X_c\}$
4. 6*NCPSUM head loads of grouped piles $\{X_t\}$.

The results obtained from GEPAN for the direct loading effect generally agree well with the other standard programs such as PIGLET and DEFPIG (Xu and Poulos, 1998). One of the most attractive advantages of the proposed 3*D*-boundary element modeling method is that externally imposed ground movements are very easily incorporated into the governing equations if the distributions of these ground movements are known. These ground movements are absorbed into the vector $\{Y_{q,e}\}$ in governing Eq. (9) and the soil displacement vector $\{Y_q\}$ at an element '*i*' is then given as;

$$\{Y_q\}=\{Y_{q,t}\}+\{Y_{q,e}\} \tag{10}$$

where $\{Y_{q,t}\}$ = soil displacement vector on element '*i*' due to pile head load on individual piles, and $\{Y_{q,e}\}$ = soil displacement vector due to external sources.

The effects of external ground movements can be considered in two ways: (1) as displacements imposed directly, based on the known ground movements, and (2) as induced stresses based on the known ground movements. In the first case, the free-field soil movements at the pile-soil interface are indicated by a vector $\{u_{soil}\}$ as shown in Eq. (11):

$$\{Y_{q,e}\}=\{u_{soil}\} \tag{11}$$

In the second case, the induced stresses are represented by a vector $\{\sigma_{soil}\}$. The corresponding soil movements due to the soil stresses are the product of the soil influence factor matrix [*SIF*] and the soil stress vector $\{\sigma_{soil}\}$ as shown in Eq. (12):

$$\{Y_{qe}\}=[SIF]\{\sigma_{soil}\} \tag{12}$$

The head displacements of individual piles can be determined from the following Eq. (13).

$$\{X_i\}=-[O]\{X_e\}+[P]\{X_b\}+[R]\{Y_p\} \tag{13}$$

In this paper, the above approaches has been adopted, and the analytical solutions presented in Eqs. (5), (6) and (7) to predict the tunnelling-induced ground movements have been incorporated directly in to Eq. (11) of the computer program GEPAN. The applicability of the programme GEPAN was verified for a case study described below.

CASE STUDY

Case histories regarding pile responses due to tunnelling are very scarce in the literature, but one useful case history is that reported by Lee et al., (1994) in which measurements of lateral pile deflections induced by a nearby tunnel construction were recorded. The case history has been analysed to investigate the validity of the computer programme GEPAN described above.

The case involves the construction of a tunnel for the Angel Underground Station in London (Chen et al., 1999). The tunnel was driven between pile foundations supporting a seven storey building with a two storey basement, the tunnel axis line being about 5.7 m from the centreline of the nearest piles. The tunnel was excavated using hand tools in two stages, the first a pilot tunnel of 4.5 m diameter and the second an enlargement of 8.25 m diameter. Measured ground loss ratios were approximately 1.5% for the pilot tunnel and 0.5% for the tunnel enlargement (Mair, 1993).

The piles were driven through 28 m of London Clay to the underlying Woolwich and Reading Beds. Ground investigation data showed that the average undrained shear strength of London Clay increased linearly from about 50 kPa at the top to about 220 kPa at the bottom. Inclinometers were installed at various locations of the ground and within some of the piles to measure the lateral soil movements and lateral pile deflections. Measured results were presented for a pile which had a diameter of 1.2 m and was located 5.7 m away from the tunnel horizontal axis line. At the pile location the depth, *h*, of the tunnel axis level was about 15 m.

Based on available data, the following assumptions were made in the analyses: (i) due to limited data available, the pile was treated as a single pile in the analyses, and (ii) average undrained shear strength $c_u=135$ kPa and soil Young's modulus $E_s=54$ MPa ($E_s=400c_u$).

The computed lateral pile deflection profiles corre-

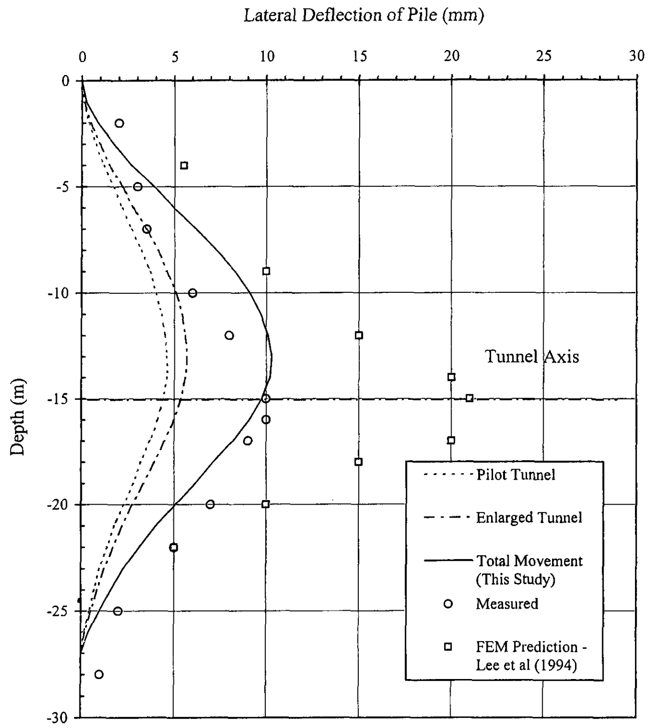

Fig. 4. Predicted and measured lateral deflections of pile adjacent to angel underground station, London (Field data and FEM predictions based on Lee et al., 1994)

sponding to each tunneling stage and the total deflection are shown in Fig. 4, together with that measured and that predicted by Lee et al. (1994). The agreement between the computed final profile and the measured is good, although the predicted maximum lateral deflection occurred slightly above the measured maximum deflection, which occurred at tunnel centreline. Therefore, it may be assumed that the computer programme GEPAN predicts the tunnelling-induced pile behaviour reasonably well. In addition, a detailed comparison study was performed using commercially available computer software FLAC^{3D}.

NUMERICAL COMPARISONS

FLAC 3*D* is a three-dimentional explicit finite-difference programme for engineering mechanics computation (Itasca, 1997). Figure 5 shows a typical tunnel-pile group configuration in this study. The configuration and the properties of the tunnel-pile group system analysed are; (i) tunnel diameter and the depth to the centreline are 6 m and 15 m. A ground loss value of 1% is considered, (ii) a 2×2 pile group, with four identical piles of 0.8 m diameter and 18 m long piles, is located horizontally 5.5 m (''front'' pile) away from the tunnel centreline, and *(iii)* the pile cap is not in contact with the soil.

Piles were modelled as structural elements and the pile-soil interaction was modelled using elastic spring constants. The stiffness of normal coupling spring, K_n, and shear coupling spring K_s were derived using the Eqs. (14) and (15) (Randolph, 1992).

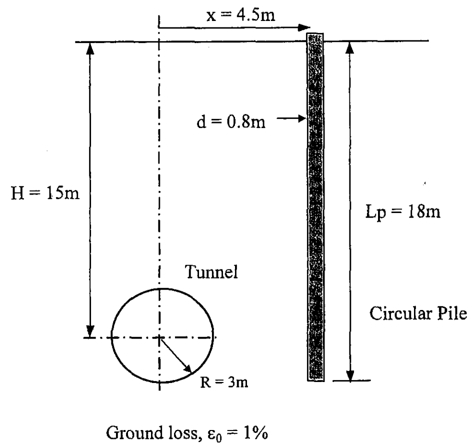

Fig. 5. Typical tunnel-pile group configuration for FLAC^{3D} analyses

Table 2. Material properties used in FLAC^{3D} analysis

Soil: Elastic model	
Bulk modulus	5×10^7 $\mathrm{Nm^{-2}}$
Shear modulus	1.07×10^7 $\mathrm{Nm^{-2}}$
Density	2000 $\mathrm{kgm^{-3}}$
Pile: Elastic model	
Young's modulus	30×10^9 $\mathrm{Nm^{-2}}$
Poisson's ratio	0.25
Cross sectional area	0.503 $\mathrm{m^2}$
Exposed perimeter	2.51 m
Second moment of inertia, $I_y=I_z$	2.0×10^{-2} $\mathrm{m^4}$
Polar moment of inertia, J	0.643 $\mathrm{m^4}$
Soil-Pile Interface: Elastic model	
Stiffness of shear coupling, K_s	1.92×10^{10} N/m/m
Cohesive strength of shear coupling, C_s	7.5×10^4 $\mathrm{Nm^{-2}}$
Friction of shear coupling, φ_s	10^0
Stiffness of normal coupling, K_n	1.6×10^{11} N/m/m
Cohesive strength of normal coupling, C_n	7.5×10^4 $\mathrm{Nm^{-2}}$
Friction of normal coupling, φ_n	0^0

$$k_n \approx 10\left(\frac{E_p}{G}\right)^{-0.14} G \tag{14}$$

$$k_s \approx 1.6G \tag{15}$$

where E_p is the Young's Modulus of solid pile and G is shear modulus of soil.

Both the cohesive strength of the shear coupling and the normal coupling were assumed to be equal to the undrained shear strength of the soil. The soil strength considered in this study was 75 kPa. The friction of the normal coupling spring for the lateral load condition was assumed to be zero.

Soil, pile and pile-soil interface parameters used in this study are given in Table 2. The in-situ stresses were assumed to be as per the K_0 condition. Once the gravitational equilibrium was reached, the tunnel excavation was carried out by applying the ''null'' model to the specified tunnel grid geometry. Since the analyses were concerned only the ultimate tunnelling-induced behaviour, applying a ''null'' model to simulate the tunnel excavation is considered to be adequate.

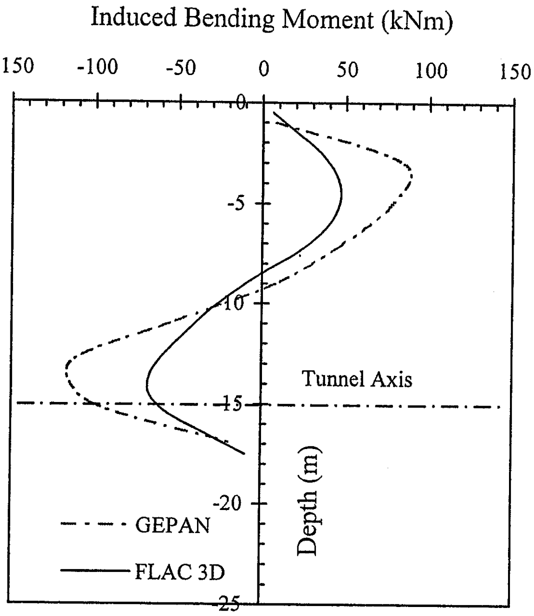

Fig. 6. Comparison of tunnelling-induced bending moment

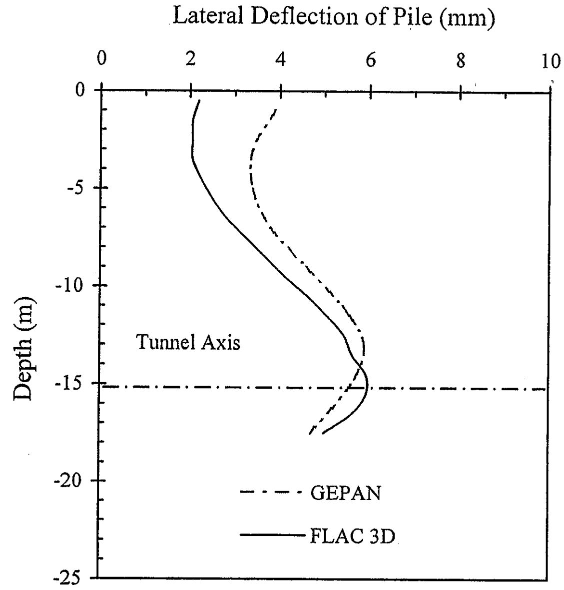

Fig. 8. Comparison of tunnelling-induced lateral deflection of pile

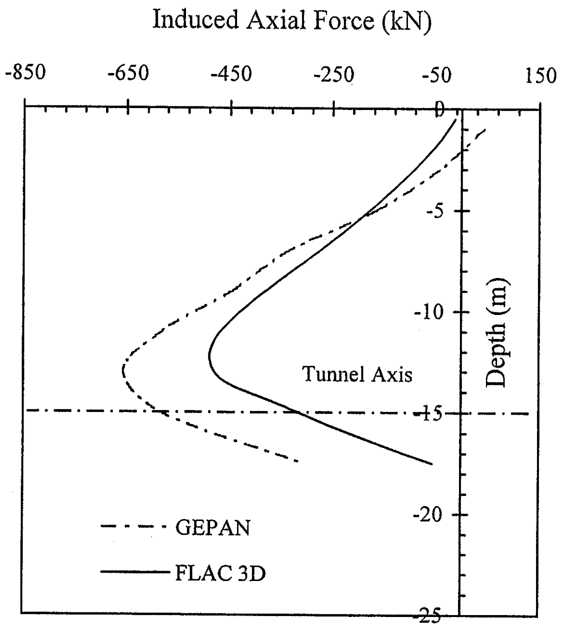

Fig. 7. Comparison of tunnelling-induced axial down drag force

Figures 6 and 7 show the predictions of tunnelling-induced bending moment and the axial downdrag force using GEPAN and FLAC 3*D*. It may be observed that although the shape of the profiles are identical, the predictions made by GEPAN over-estimate the bending moment and the axial down drag force. Figure 8 shows the comparison of the lateral deformation of the pile. The maximum lateral deformation predicted by both GEPAN and FLAC 3*D* are almost the same. However, the pile head deflection predicted by GEPAN is larger than the FLAC 3*D* prediction. The reasons for the difference in predictions may be due (i) Tunnelling-induced deformation pattern predicted by both programmes are different due to the difference in the displacement modelling technique, and (ii) The empirical formulae used in FLAC 3*D* to model the pile-soil interface were derived from the equivalent 2*D* problem, which may not model the 3*D* problem accurately.

An accurate assessment of the influence of tunnelling adjacent to an existing pile foundation is possible only by using 3*D* numerical analysis with an appropriate soil model. Three 3*D* numerical tools were studied in this analysis, a 3*D* boundary element computer programme, GEPAN (Xu and Poulos, 1998) and a 3*D* finite difference programme FLAC 3*D* (Itasca, 1997). The results of these analyses were compared by performing single pile and pile-group analyses. In general, both programmes predicted broadly similar tunnelling-induced pile behaviour.

Although the GEPAN programme over-estimated the tunnelling-induced behaviour, it is very computer-cost-effective. Computer running times for an identical problem using GEPAN and FLAC 3*D* were about 2 minutes and about 10 hours respectively using a computer with 196 MB RAM. In addition, unlike in FLAC 3*D*, GEPAN programme require only relatively few soil and pile parameters.

A parametric study on the effect of tunnelling-induced ground movements on the adjacent piles and pile groups is presented below using GEPAN computer programme.

TUNNELLING-INDUCED PILE-GROUP RESPONSES

Analyses

Figure 9 illustrates the general problem addressed in this paper, where an existing 2×2 pile group is situated adjacent to a tunnel under construction. Piles in the group are spaced at $3d$, where d is pile diameter. The Young's modulus of pile, $E_p = 30{,}000$ MPa and the Pois-

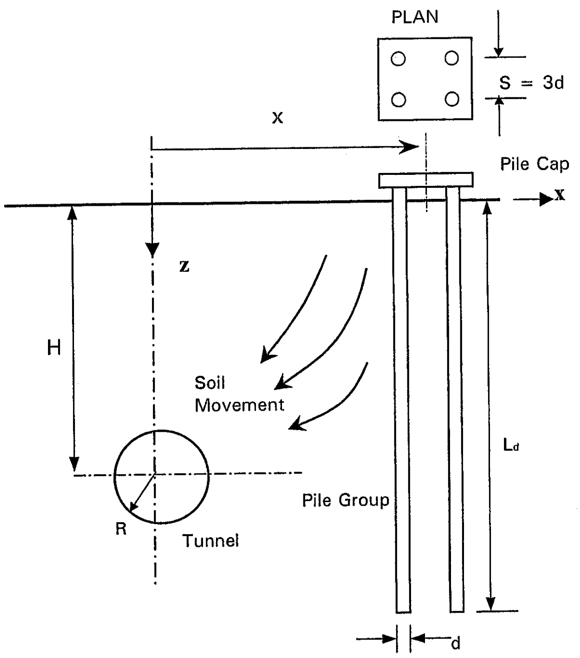

Fig. 9. Pile group adjacent to tunnelling—the basic problem analysed

son's ratio, $\nu=0.25$. All four piles in the pile group are assumed to be fixed against rotation at the pile cap. A uniform isotropic subsurface soil profile is assumed in the analysis with constant soil strength, $c_u=60$ kPa. The soil modulus is calculated using the relationship, $E_s=400$ c_u and a Poisson's ratio (ν) of 0.5 is assumed, representing undrained conditions. The soil layer thickness is assumed to be infinite. Interaction between the pile cap and the ground surface is not considered in the present analysis.

Tunnelling will generally induce both vertical and horizontal components of ground movements. The vertical ground movement above the tunnel's horizontal axis is generally downward and will impose negative skin friction on the pile, causing pile settlement and a possible reduction in the effective pile load carrying capacity. The horizontal soil movement tends to be towards the tunnel axis and will induce additional lateral deflection and bending moment in the pile.

The analyses of pile group and single pile responses have been carried out using the computer programme GEPAN. Only elastic behaviour of the pile and the soil has been considered in this analysis. The following analysis have been performed in order to assess the effect on adjacent piles due to tunnelling-induced ground movements:

1. Assessment of induced bending moment, axial forces, lateral deformation and the lateral deformations on piles in a 2×2 pile group consisting of 0.8 m diameter and 25 m long bored piles. The horizontal distance between the front row piles and the tunnel centerline is 4.5 m. The depth of tunnel (centerline) from the surface is 20 m and the tunnel diameter is 6 m. Analyses have been repeated for identical single piles horizontally located at the same distances as the piles in the group in order to compare the pile behaviours both as single piles and within the group. Analyses have been carried out for a typical ground loss value of 1%.
2. Assessment of the pile group behaviour for different horizontal distances from the tunnel centerline. The centre of the pile group is assumed to be located 5.7 m from the tunnel axis.
3. Assessments of the pile group behaviour for different pile lengths. The depth of tunnel (centerline) from the surface is 20 m and the tunnel diameter is 6 m. Analyses have been carried out for a ground loss value of 1%.

RESULTS AND DISCUSSIONS

Figure 10 shows a comparison of the computed settlement profiles of piles in the pile group and single piles at an equal horizontal distance from the tunnel centerline. The settlement of the "front" piles is slightly higher than the settlement of "rear" piles since the tunnelling-induced settlements decrease as the distance from the tunnel decreases. The settlement of single isolated piles at equivalent distances from the tunnel is slightly higher than the piles in the group. The settlement profiles with depth for both a single pile and a pile in the group are almost identical. Therefore, the tunnelling-induced settlement behaviour of single piles appears to be reasonably representative of the settlement behaviour of piles in a group.

Figure 11 shows a comparison of the tunnelling-induced lateral deformation profile of piles in the pile group and single piles at identical horizontal distances from the tunnel. As expected, the lateral deformation of the "front" piles (closer to tunnel) in the group is higher than for the "rear" piles, and the maximum lateral deformation occurs at a depth equal to that of the tunnel center. The lateral deformation profile for single piles is almost identical to that of the piles in a group.

Figure 12 shows a comparison of the tunnelling-induced bending moment profile of piles in a group and single piles at equivalent distances. The maximum bending moment occurs at about the tunnel axis depth level. The bending moment profile for piles in a group and single pile are almost the same, except for a small difference at the pile cap location due to the fixity condition. Thus, the bending moment profile obtained for single piles gives a reasonable representation of the profile for a pile in a group.

Figure 13 compares the induced axial force profiles for piles in a group and a single pile at an equal distances from the tunnel. The axial down-drag force estimated for a single pile is about 20% higher than the down-drag force induced in a pile within the pile group. This indicates that pile group effect reduces the induced axial down-drag forces on a pile in the group, and this observation is consistent with the findings of Kuwabara and Poulos (1989).

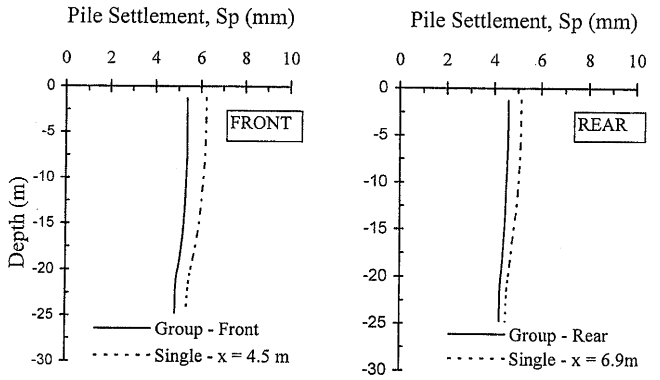

Fig. 10. Comparison of the settlement of a pile in a group and a single pile at equal distance from the tunnel axis

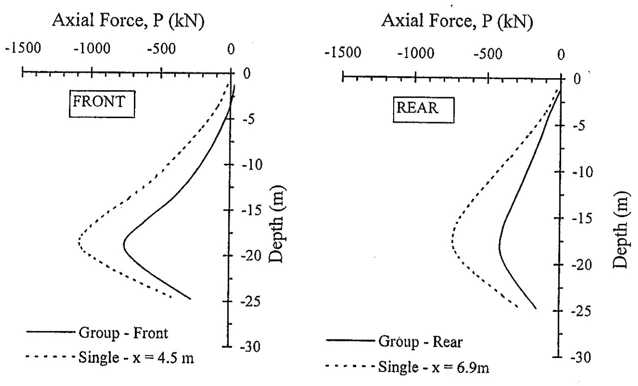

Fig. 13. Comparison of the induced axial forces on a pile in a group and a single pile

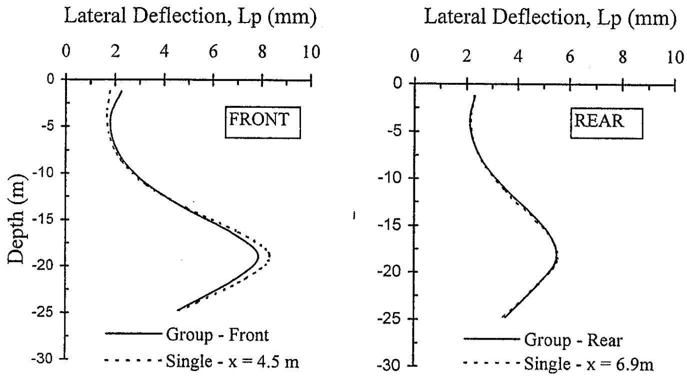

Fig. 11. Comparison of the lateral deformation of a pile in a group and a single pile

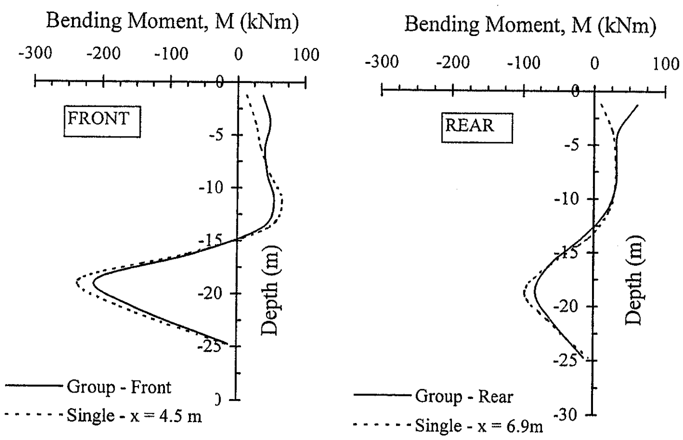

Fig. 12. Comparison of the induced bending moment on a pile in a group and a singie pile

The above calculations indicate that a relatively simple single pile analysis can be used to predict the tunneling-induced bending moment, lateral deformation and settlement in a pile group at identical distances from the tunnel. However, the tunneling-induced axial down-drag force estimated for single pile may be larger than for a pile in a pile group. Figure 14 shows a comparison of the settlement, lateral movement and rotation of a pile group (at the pile cap), a single pile (at the pile head), and the ground surface, for varying horizontal distances from the tunnel. It is observed that the settlement and the lateral deformation of the pile group and single pile are identical for varying horizontal distances but are less than the ground surface settlement and lateral deformation. The maximum values of both lateral deformation and the rotation of the pile head occur at a horizontal distance equal to the ground surface settlement trough width, *i*. The rotation at ground level for a single pile is less than the rotation of pile cap. This is due to the difference in pile head fixity conditions of the single pile and the group pile. The ground surface rotates more than either the single pile or the pile group.

Figure 15 shows a comparison of "front" and "rear" pile behaviour of a 2×2 pile group, for varying pile lengths. Pile head settlement and the lateral deflection are large when the pile tip is located around tunnel depth level, and the "front" pile laterally deflects more than the "rear" pile. When the pile tip is located below the tunnel, the pile head settlement reduces. The maximum down-drag force and the maximum bending moment are high when the pile tip is located at tunnel invert level, and there is little variation in maximum down-drag force and the bending moment values when the pile tip becomes deeper and is below the tunnel invert level.

CONCLUSIONS

In this paper, an analytical method proposed by the authors is used to estimate the tunnelling-induced ground movements. The analytical formulae presented in this paper (Eqs. (5), (6) and (7)) may be used to assess tunnelling-induced ground deformations, both surface and sub-surface. These equations allow rapid estimation of the ground deformations and require only an estimate of the Poisson's ratio, ν, of the soil. The settlement trough width '*i*' parameter presented in this paper (Eq. (8)) compares well with the existing empirical and analytical formulae.

In urban areas, ground movements induced by tunnelling can have an influence on nearby pile foundations. The analytical solutions for tunnelling-induced ground

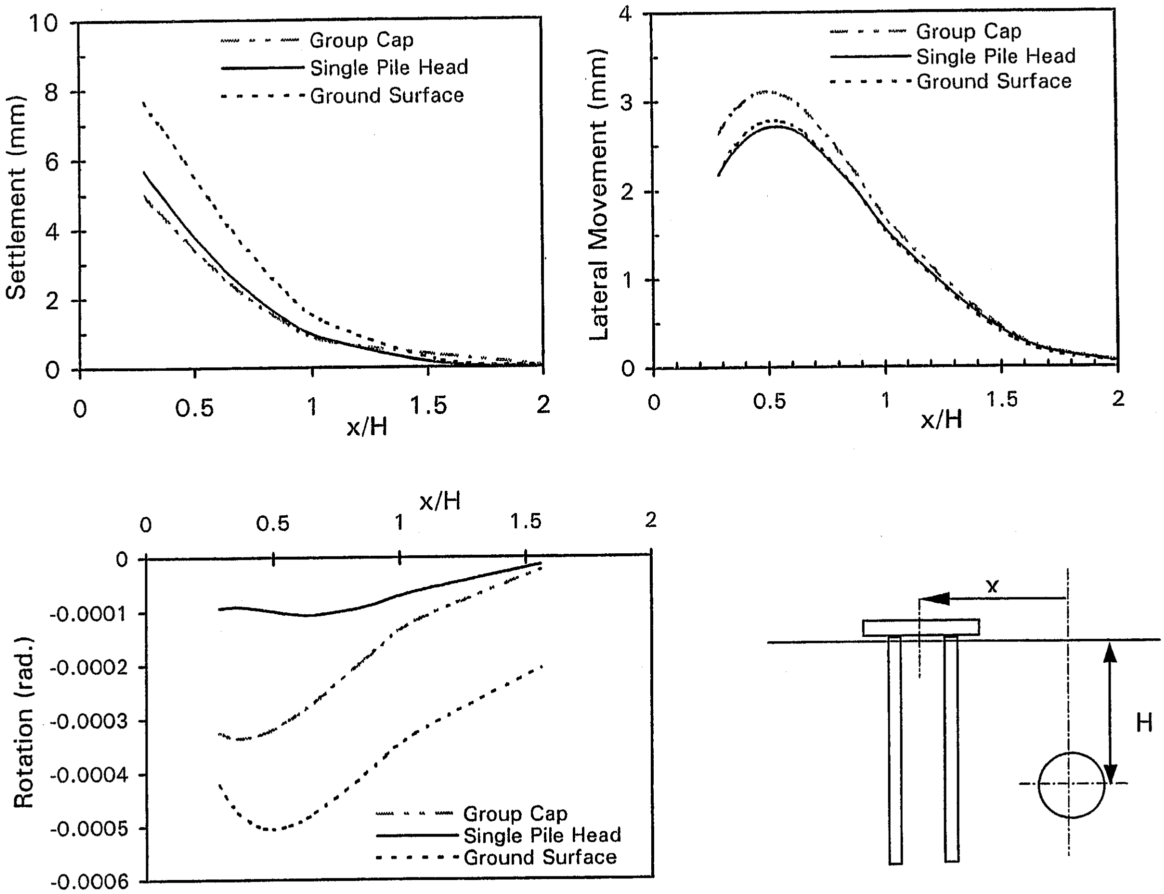

Fig. 14. Comparison of single pile head, pile group cap and ground surface movements

movements have been incorporated into the computer programme GEPAN to compute the response of a pile group and single piles. The case study presented and the numerical comparisons using FLAC 3*D* showed that the predictions using GEPAN were reasonable.

A 2 × 2 pile group has been analysed for varying lateral distance from the tunnel. The behaviour of a pile in the group has been compared with the behaviour of an identical single pile. The effect of varying pile lengths with respect to the tunnel depth has also been studied.

The study shows that a single pile analysis can predict adequately the tunneling-induced bending moment, lateral deformation and settlement for a pile in a pile group, at an identical distance from the tunnel. However, the tunneling-induced axial down-drag force estimated for single pile is about 20% higher than for a pile in a pile group, in this study. Significant pile settlement and lateral deformation are induced when the pile tip located at about the tunnel depth level. Similarly the induced down drag and bending moment are significant when the pile tip is located at the tunnel invert level.

As a first approximation, the tunnelling-induced additional bending moments, lateral deflections, settlements and the rotations on piles may be added to the original design values due to structural loading when making an assessment of the potential for pile overstressing due to tunnelling operation.

ACKNOWLEDGEMENTS

The work presented in this paper forms part of a project on "Effect of Tunnelling and Underground Construction on Pile Foundations" supported by a grant from The Australian Research Council (ARC).

REFERENCES

1) Beneerjee, P. K. and Driscoll, R. M. C. (1976): Three-dimensional analysis of raked group, *Proc., Inst. Civil*, (61) 653–671.
2) Clough, G. W. and Schmidt, B. (1981): Excavations and Tunnelling, Chapt. 8 in Soft Clay Engineering, Brand, E. W. and Brenner, R. P. (eds.) Elsevier.
3) Chen, L. T., Poulos, H. G. and Loganathan, N. (1999): Pile responses due to tunnelling, *ASCE Geotech. J.*
4) Cording, E. J. and Hansmire, W. H. (1975): Displacement around soft ground tunnels, General Report: Session IV, Tunnels in Soil, *Proc. of 5th Panamerican Congress on SMFE.*
5) Deane A. P. and Bassett R. H. (1995), The Heathrow Express trial tunnel, *Proc. Institution of Civil Engineers*, Geotechnical Engineering, **113**, July, 144–156.
6) Gunn, M. J. (1993): The prediction of surface settlement profiles due to tunnelling, Predictive Soil Mechanics, *Proc. of the Wroth Memorial Symp.*, Houlsby, G. T. and Schofield, A. N. (eds.) Oxford, 304–316.
7) Itasca (1997): *FLAC^{3D} User Manuel*, Itasca Consulting Group, USA.
8) Kuwabara, F. and Poulos, H. G. (1989): Downdrag forces in a group of piles, *J. Geotech. Engrg. Div.*, ASCE, **115** (GT6), 806–

818.

9) Lee, R. G., Turner, A. J. and Whitworth, L. J. (1994): Deformations caused by tunnelling beneath a piled structure, *Proc. 13th ICSMFE*, New Delhi, India, 873–878.

10) Loganathan, N. and Poulos, H. G. (1998), Analytical prediction for tunnelling-induced ground movements in clays, *J. of Geotech. and Geoenv. Engrg.*, ASCE, **124** (9).

11) Loganathan, N. and Poulos, H. G. (1999): Tunneling-induced ground deformations and their effect on adjacent foundations, *The Race For Space-10th Australian Tunnelling Conf.*, Melbourn, Australia, March 1999.

12) Mair, R. J. (1993): Ground movements around shallow tunnels in soft clay, 10th ICSMFE Stolkhom, 323–328.

13) O'Reilly, M. P. and New, B. M. (1982): Settlements above tunnels in the U.K.-their magnitude and prediction, *Tunnelling '82*, 173–181.

14) Peck, R. B. (1969), Deep excavations and tunnelling in soft ground, *Proc. of 7th ICSMFE*, Mexico City, 225-290.

15) Poulos, H. G. (1979): An approach for the analysis of offshore pile group, *Proc. Conf. On Numerical Methods in Offshore Piling*, Inst. Of Civil Engrg, London, 119-126.

16) Poulos, H. G. (1990): DEFPIG users guide, *Center for Geotechnical Research*, University of Sydney, Australia.

17) Randolph, M. F. (1980): PIGLET: A computer programme for the analysis and design of pile groups under general loading conditions, *Soil Report TR91*, CUED/D, Cambridge Univ., Cambridge, England.

18) Rowe, R. K. and Kack, G. J. (1983): A theoretical examination of the settlements induced by tunnelling: Four case histories, *Can. Geotech. J.*, **20**, 299–314.

19) Sagaseta, C. (1987): Analysis of undrained soil deformation due to ground loss, *Géotechnique*, **37**, 301–320.

20) Stallebrass, S. E., Grant, R. J. and Taylor, R. N. (1996): A finite element study of ground movements measured in centrifuge model tests of tunnels, *Proc., Int. Symp. On Geotech. Aspects of Underground Constr. In Soft Ground*, Mair, R. J. and Tailor, R. N. (eds.), A. A. Balkema, Rotterdam, The Netherlands.

21) Taylor, R. N. (1998): Modelling of tunnel behaviour, *Proc. Inst. Civil Engineers, Geotech. Engrg*, UK, **131**, 127–132.

22) Verruijt, A. and Booker, J. R. (1996): Surface settlements due to deformation of a tunnel in an elastic half plane, *Géotechnique*, **46**(4), 753–756.

23) Xu, K. J. and Poulos, H. G. (1998): General elastic analysis of piles and pile group, *Int. J. For Numerical and Analytical Methods in Geomechanics* (Under review).